CHINESE JOURNAL OF MECHANICAL ENGINEERING
Vol. 23, No. *, 2010

DOI: 10.3901/CJME.2010.**.***, available online at www.cjmenet.com; www.cjmenet.com.cn

Self- sustained Oscillation Pulsed Air Blowing System for Energy Saving

CAI Maolin* and XU Weiqing

School of Automatic Science and Electrical Engineering, Beihang University, Beijing 100191, China

Received June 9, 2009; revised April 1, 2010; accepted April , 2010; published electronically April , 2010

Abstract: Currently, many studies have been made for years on dimensions of pneumatic nozzle, which influence the flow characteristic of blowing system. For the purpose of outputting the same blowing force, the supply pressure could be reduced by decreasing the ratio of length to diameter of nozzle. The friction between high speed air and pipe wall would be reduced if the nozzle is designed to be converging shape comparing with straight shape. But the volume flow and pressure, discussed in these studies, do not describe energy loss of the blowing system directly. Pneumatic power is an innovative principle to estimate pneumatic system's energy consumption directly. Based on the above principle, a pulse blowing method is put forward for saving energy. A flow experiment is carried out, in which the high speed air flows from the pulse blowing system and continuous blowing system respectively to a plate with grease on top. Supply pressure and the volume of air used for removing the grease are measured to calculate energy consumption. From the experiment result, the pulse blowing system performs to conserve energy comparing with the continuous blowing system. The frequency and duty ratio of pulse flow influence the blowing characteristic. The pulse blowing system performs to be the most efficient at the specified frequency and duty ratio. Then a pneumatic self-oscillated method based on air operated valve is put forward to generate pulse flow. A simulation is made about dynamic modeling the air operated valve and calculating the motion of the valve core and output pressure. The simulation result verifies the system to be able to generate pulse flow, and predicts the key parameters of the frequency and duty ratio measured by experiment well. Finally, on the basis of simplifying and solution of the pulse blowing system's mathematic model, the relationship between system's frequency duty ratio and the dimensions of components is simply described with four algebraic equations. The system could be designed with specified frequency and duty ratio according to the four equations. This study provides theoretical basis for designing energy-saving air blowing system.

Key words: energy saving, pulse blowing, self-sustained oscillation, pneumatic power

Notations

p—Absolute pressure, Pa;
p_s—Supply pressure of nozzle, Pa;
p_{work}—The lowest pressure of chamber II and III , Pa;
Δp —Differential pressure needed for air operated valve to switch, Pa;
ρ_0—Density (Atomosphere Normale De Reference, ANR), kg/m^3;
θ—Temperature, K;
θ_0—Temperature (ANR), K;
Q —Air volume flow, m^3/s;
G —Air mass flow, kg/s;
R—Ideal gas constant, J/(K•mol);
κ—Adiabatic index,
S_e—Effective area, m^3;
C —Sonic conductance (proportional to area of orifice), dm^3/(s • MPa);
t—Time, s;
t_r—Reference time, s;
T —Period, s;
t_{rsp}—Response time of air operated valve, s;
f —Frequency, s;
α —Duty ratio.

Subscript

u—Upstream, d—Downstream, a—Atmosphere, 1—Chamber I, 2—Chamber II, 3—Chamber III, i—Inflow, o—Outflow.

1 Introduction

Air blowing system is widely utilized in many fields of industry. It is used primarily for scrap removal, as well as drying and cooling. It's inevitable that some kinds of scrap and water drops are left between processes, this system is the handiest tool to blow off them quickly without stopping the line, such as cleaning a conveyor at a metal processing facility to remove small scrap buildup, drying the water

* Corresponding author. E-mail: caimaolin@gmail.com

drops in parts and cooling in the last process. Compressed air in pneumatic systems was costly to create and the blowing system consumed half of the total air created in the industries of machining[1]. One question about using the compressed air for blowing is the large energy consumption. Many studies have been made to reduce energy waste. ONEYAMA[2] described the present station and project on energy conservation of pneumatic system. In Ref. [3], it is discovered that the existing air blowing system requires double compressed air of more efficient types. So it is meaningful to investigate the blowing system to improve its efficiency.

The characteristic of water jet system for cleaning has been studied for many years, CHAHINE, et al[4], verified that pulse water jet could enhance the ability to remove aircraft coatings. They developed self-resonating jet nozzle based on Helmholtz oscillator[5]. Their comparative testing had shown that self-resonating cavitating jets could perform underwater cleaning more effectively than conventional jets. WANG, et al[6], developed a low pressure and large flow pulsation-jet nozzle for cleaning oil tank bottom sludge. They explained the generation mechanism, which was different from a high pressure and low flow pulsation-jet.

The study in characteristic of air blowing system has been started in recent years. Researches find that blowing wastes a huge amount of compressed air. SENOO[7] and KOKOROZASI[8] proposed several methods of rational utilizing air blow in the industries for reduction of air consumption. ONEYAMA[9] showed the dimensions (length and diameter) of an air blow influence supply pressure of the system to output a same blowing force. It was verified that the supply pressure could be reduced when the ratio of length to diameter decreased, which meant pressure loss became less. In the study, the characteristics of air blows of different shapes were considered and the converging blow with the shape that the area of exit was much smaller than entrance achieved the lowest pressure loss. YANG, et al[10], investigated the effects of nozzle shape, the curvature, Reynolds number and the spacing between the nozzle exit and the blown surface, which influenced the distribution of velocity of air blowing out.

But in these studies, most discussion focused on the volume flow and pressure which are parameters that do not describe energy loss of the blowing system directly. Pneumatic power is an innovative principle to estimate pneumatic system's energy consumption directly. This paper describes the mechanism of energy loss in conventional air blowing system with the principle. Generally air flows to nozzle through pressure regulator in many industries. Pressure drops from 0.6–0.8 MPa (absolute pressure) in air supply to 0.2–0.4 MPa in nozzle with available energy[11] lost about 39%–47%.

The paper presents an innovative air blowing system generating pulse jets with a self-oscillated device instead of the pressure regulator. The pulse jets are proved to perform more effectively than continuous blowing. Then the pulse frequency and duty ratio are studied to influence blowing efficiency. For industrial application, a pneumatic self-oscillated system based on air operated valve is presented and the simulation well predicts the key parameters of frequency and duty ratio. Finally, a method is developed to design the pulse frequency and duty ratio of the system.

2 Energy Saving Scheme

2.1 Mechanism of energy loss

Fig. 1(a) shows air blowing system in many industries. Air flows from air supply through pressure regulator to the nozzle. Table 1 shows the condition of nozzle used in industries.

Table 1. Condition of nozzle used in industries

Parameter	Value
Supply pressure of the system p_{s0} /MPa	0.6–0.8
Supply pressure of the nozzle p_s /MPa	0.3
Pressure of atmosphere p_a /MPa	0.1

According to the equation of pneumatic power[12], the pneumatic power of the upstream and downstream is obtained respectively:

$$P_u = p_{s0} Q_{s0} \ln \frac{p_{s0}}{p_a}, \tag{1}$$

$$P_d = p_s Q_s \ln \frac{p_s}{p_a}. \tag{2}$$

With the equation of continuity, the following is obtained:

$$\rho_{s0} Q_{s0} = \rho_s Q_s. \tag{3}$$

So the equation below is obtained:

$$\frac{P_s}{P_{s0}} = \frac{\ln \frac{p_s}{p_a}}{\ln \frac{p_{s0}}{p_a}} = 53\%–61\% \tag{4}$$

Eq. (1) shows the energy of the air decreases by 39%–47% when the air flows through the pressure regulator. For the purpose of avoiding energy loss at the pressure regulator, the innovative energy saving device is proposed as Fig. 1(b) shows. The PLC outputs pulse signals to drive solenoid valve to switch, and then the nozzle outputs pulse flow. So the nozzle's upstream pressure rises

from p_s to p_{s0}, and the energy loss at pressure regulator is avoided. But the instantaneous volume flow increases. The pneumatic power increases as well. To reduce the average volume flow the duty ratio is set to be small. Pneumatic power could become small with this method.

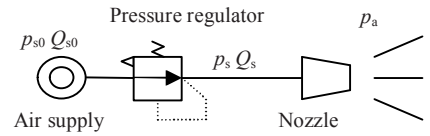

(a) Conventional air blowing system

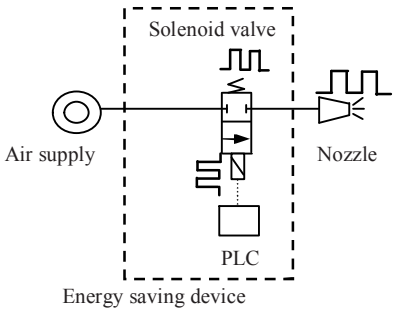

(b) Innovative air blowing system

Fig. 1. System comparison

In the next section, it will be discussed that the relationship among frequency, duty ratio of the pulse flow, and the air consumption of the system for blowing away particles.

2.2 Experimental study on characteristic of the air pulse blowing system

The purposes of the experiment are made as follows: (1) To prove the pulse blowing system saving energy comparing with continuous blowing; (2) To study how the frequency and duty ratio influence the air consumption for blowing away particles.

2.2.1 Scheme of experiment

The scheme of the experiment is described as follows.

(1) Modeling the particles on the surface of work. The particles (mixture of water and oil) are removed quickly while the high-speed airflow is blowing. So it is needed to modeling the particles, because the period of particles removing is too short to measure. Grease is verified to be a kind of appropriate material. On the one hand it is a kind of viscous material as same as the particles, on the other hand it is easy to measure the period.

(2) Description of blowing process. Fig. 2(a) shows the thickness of the grease layer becomes thinner and thinner gradually while the air is blowing.

(3) Measurement of the quantity of particles removed. Fig. 2(b) shows the light signal sent from the light emitting diode(LED) penetrates the grease layer to the phototransistor, and then the phototransistor is turned on. Light intensity is proportional to output (U_0) of the phototransistor approximately and inverse to thickness of the grease layer left. The output of the phototransistor is approximately proportional to the thickness of the grease layer blown away. U is defined as the ratio of U_0 to reference output of phototransistor to describe the quantity of particles removed. Fig. 2(c) shows the relationship between the quantities of particles removed and air consumption in the blowing process.

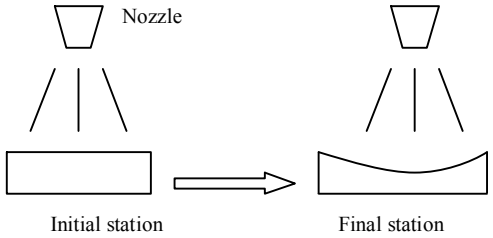

(a) Variation of grease layer

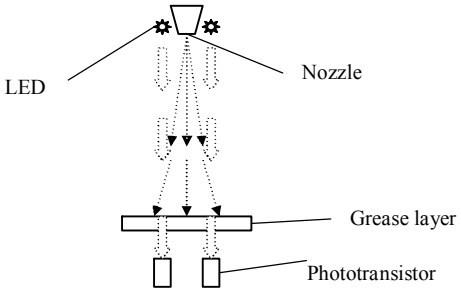

(b) Measurement principle

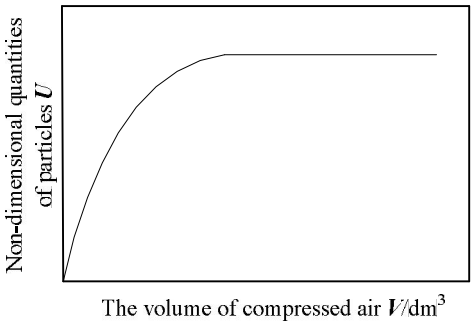

(c) Relationship between the quantities of particles removed and air consumption

Fig. 2. Experiment principle

2.2.2 Experiment result

The experiment result can be obtained as follows.

(1) Frequency (f). Fig. 3(a) shows the characteristic curves at different frequencies. Different volumes of air (V) are consumed at different frequencies to blow away the same quantities of particles (U=0.8). The pulse blowing in higher pressure condition (p_s=0.5 MPa) consumes smaller volume of air comparing with continuous blowing in lower pressure condition (p_s=0.3 MPa). The pulse blowing consumes the smallest volume (42% volume of continuous

blowing) when the frequency reaches 10 Hz.

(2) Duty ratio (α). In this section, the influence of the duty ratio to air consumption will be discussed.

Figs. 3(b)–3(d) shows the system characteristic when duty ratio is changed at frequency of 10 Hz. In Fig. 3(b), it consumes the smallest volume (26% volume of continuous blowing) when the duty ratio reaches to 40% to blow away a same quantity of particles (U=0.8). In Fig. 3(c), it consumes the smallest volume (29% volume of continuous blowing) when the duty ratio reaches to 50%. In Fig. 3(d), it consumes the smallest volume (27% volume of continuous blowing) when the duty ratio reaches to 40%.

As Fig. 3(e) shows, industry condition (continuous blowing p_s=0.3 MPa) is defined as reference condition. V_0 is the volume of air consumed to blowing away 0.8 particles (U=0.8) in the reference condition and t_0 is the time consumed. It can be seen that V/V_0 (t/t_0) varies depending on p_s and α (duty ratio). V/V_0 is reduced to 30% and t/t_0 to 15%(Fig. 3(f)) when p_s increases, which means 70% of the air and 85% of time are conserved when duty ratio is 40% and p_s is 0.7 MPa.

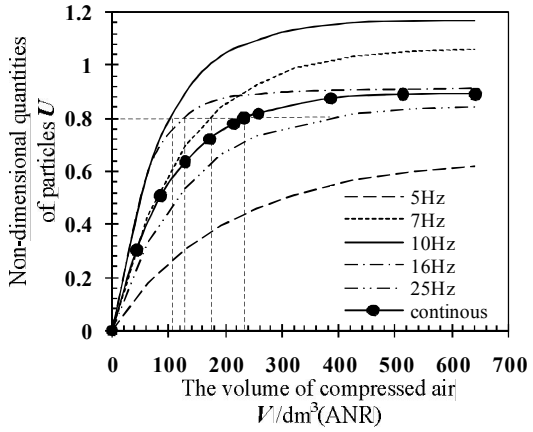

(a) System characteristic when frequency is changed

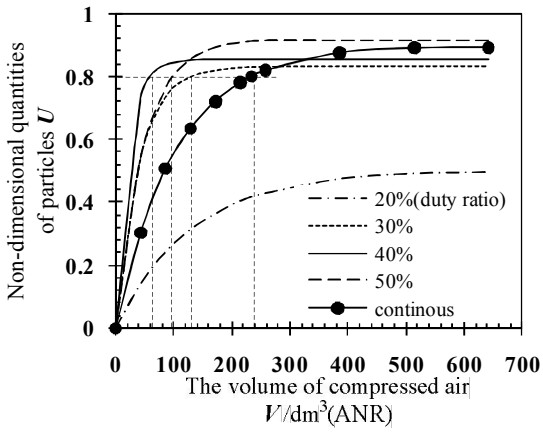

(b) System characteristic when duty ratio is changed (p_s=0.5 MPa, f=10 Hz)

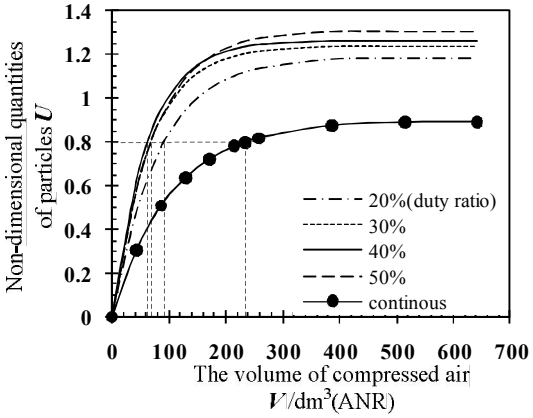

(c) System characteristic when duty ratio is changed (p_s=0.6 MPa, f=10 Hz)

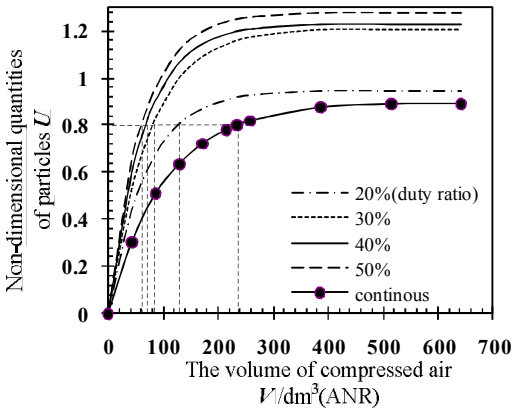

(d) System characteristic when duty ratio is changed (p_s=0.7 MPa, f=10 Hz)

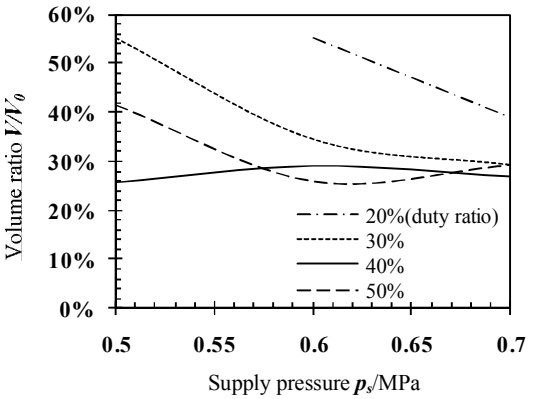

(e) Comparing the air consumption in pulse blowing conditions with continuous blowing condition

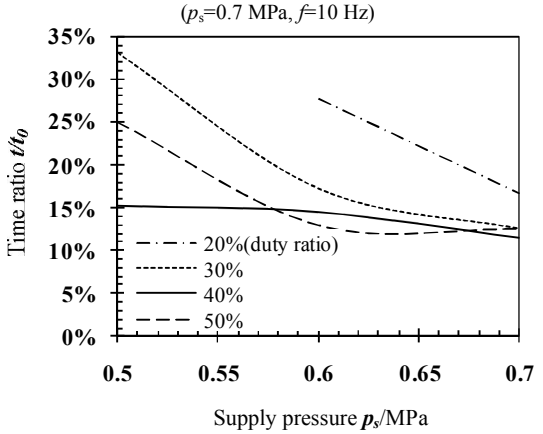

(f) Comparing the time consumption in pulse blowing conditions with continuous blowing condition

Fig. 3. Experiment results

3 Energy Saving Device

As mentioned above, the PLC is applied to drive the solenoid valve to generate pulse flow. It is so complicated that is not convenient to be applied in industry. So in this section a pneumatic self-oscillated system is discussed.

3.1 Principle of self-oscillated system

As Fig. 4(a) shows, in the start, the air operated valve stays at right position, the air flows from the air supply to port *B* then is divided into two branches, one flow to nozzle and the other to operating port *G* through throttle 1. So the pressure of the left operating chamber starts to rise, meanwhile the air in the right operating chamber flows from the throttle 3 to the atmosphere. The pressure of right operating chamber dropping, then the differential pressure between right and left operating chamber becomes large gradually. When it reaches to Δp the air operated valve switches to the left position. Then the air flows from the air supply into the right operating chamber through port *A*. So the pressure of the right operating chamber raises, meanwhile the air in the left operating chamber flows into atmosphere through throttle 2 and nozzle. The pressure of it dropping, then the differential pressure between right and left operating chamber becomes large gradually. When it reaches to Δp the air operated valve switches to the right position. So self-oscillation is achieved by this process's cycling.

Fig. 4(b) is the picture of the system. The red pipes are the pipe *BC*, *CD*, and *CE* in Fig. 4(a). The white pipe is the pipe *AJ*. The left side branch has two throttles. The right side branch has one throttle. On the top, a throttle is used to regulate effective area of outlet of the system, standing for nozzle in Fig. 4(a). All the pipes are connected to a 2 positions 5 ports operated valve. The valve is driven by compressed air. When the differential pressure of side ports becomes large, the valve switches.

3.2 Simulation and experiment

3.2.1 System model

To simplify the system, the following assumptions are made: (1) anywhere in a pipe has an equal pressure, (2) isothermal state, (3) the valve switches at uniform velocity.

Fig. 5(a) shows the model of the system in Fig. 4 when the air operated valve switches to the right position. The arrows show flow direction. Chamber I stands for pipe *BC*, *CD* and *CE* in Fig. 4, chamber II stands for pipe *FG*, chamber III stands for pipe *AH*. C_{1i} is the flow conductance into chamber I and C_{2i} is chamber II . C_{1o} is the flow conductance out chamber I and C_{3o} is Chamber III . The channel between the air supply and chamber III is cut off. Fig. 5(b) shows the model of the system when the air operated valve switches to the left position. C_{3i} is the flow conductance into chamber III , C_{2o} is the flow conductance out chamber II .The channel between the air supply and chamber I is cut off.

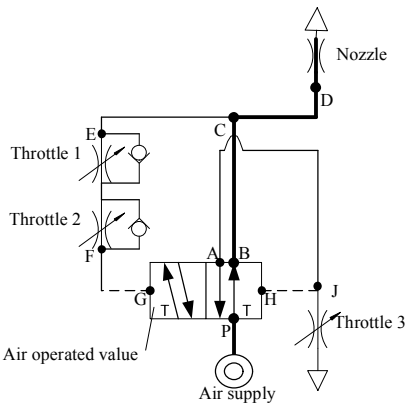

(a) Schematic diagram

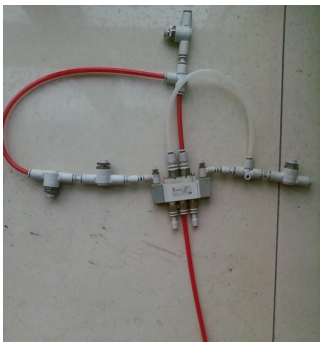

(b) Picture of the system

Fig. 4. Self-oscillated system

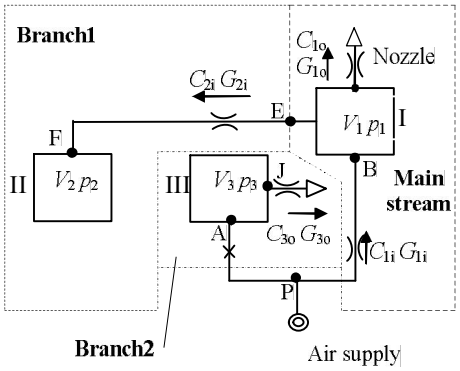

(a) Model for the right position

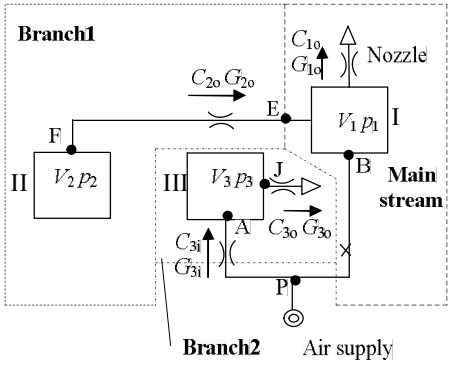

(b) Model for the left position

Fig. 5. System model

Fig. 6 shows the variation of pressure in chambers I, II, III. One cycle can be divided into four periods (*a*, *b*, *c*, *d*), i.e., periods *a* and *b* when the valve in the right position, and periods *c* and *d* when the valve in the left position.

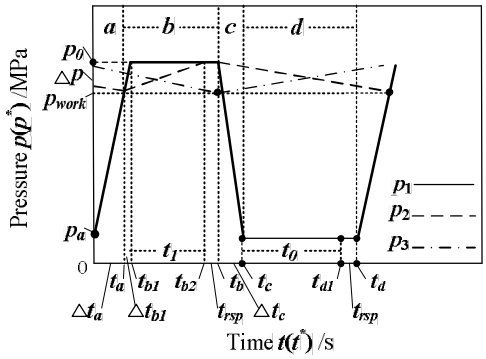

Fig. 6. Description of pressure variation of the system

Pressure change at each chamber can be obtained by differentiating the state equation of ideal gases in isothermal state:

$$\frac{\mathrm{d}p}{\mathrm{d}t}=\frac{R\theta}{V}G. \tag{5}$$

The equation of air mass flow through an orifice[12] is

$$G=\begin{cases} S_{\mathrm{e}}p_{\mathrm{u}}\sqrt{\dfrac{\kappa}{R\theta_{\mathrm{u}}}\left(\dfrac{2}{\kappa+1}\right)^{\frac{\kappa+1}{\kappa-1}}}, & \dfrac{p_{\mathrm{d}}}{p_{\mathrm{u}}}\le 0.528, \\ S_{\mathrm{e}}p_{\mathrm{u}}\sqrt{\dfrac{2\kappa}{R\theta_{\mathrm{u}}(\kappa-1)}\left[\left(\dfrac{p_{\mathrm{d}}}{p_{\mathrm{u}}}\right)^{\frac{2}{\kappa}}-\left(\dfrac{p_{\mathrm{d}}}{p_{\mathrm{u}}}\right)^{\frac{\kappa+1}{\kappa}}\right]}, & \dfrac{p_{\mathrm{d}}}{p_{\mathrm{u}}}>0.528. \end{cases} \tag{6}$$

Eq. (7) can be written as follows which is wildly used in pneumatic simulation

$$G=\begin{cases} \rho_0 C p_{\mathrm{u}}\sqrt{\dfrac{\theta_0}{\theta_{\mathrm{u}}}}, & \dfrac{p_{\mathrm{d}}}{p_{\mathrm{u}}}\le 0.5, \\ \rho_0 C p_{\mathrm{u}}\sqrt{\dfrac{\theta_0}{\theta_{\mathrm{u}}}}\cdot 2\sqrt{\dfrac{p_{\mathrm{d}}}{p_{\mathrm{u}}}\left(1-\dfrac{p_{\mathrm{d}}}{p_{\mathrm{u}}}\right)}, & \dfrac{p_{\mathrm{d}}}{p_{\mathrm{u}}}>0.5. \end{cases} \tag{7}$$

In period *a* in Fig. 6, air flows from chamber II to chamber I because the pressure of chamber II is higher than chamber I. The pressure change at chambers I, II, III are described as follows:

$$\frac{\mathrm{d}p_1}{\mathrm{d}t}=\frac{R\theta_1}{V_1}\left(G_{1\mathrm{i}}-G_{1\mathrm{o}}+G_{2\mathrm{o}}\right), \tag{8}$$

$$\frac{\mathrm{d}p_2}{\mathrm{d}t}=\frac{R\theta_2}{V_2}\left(-G_{2\mathrm{o}}\right), \tag{9}$$

$$\frac{\mathrm{d}p_3}{\mathrm{d}t}=\frac{R\theta_3}{V_3}\left(-G_{3\mathrm{o}}\right). \tag{10}$$

In period *b*, p_1 rises beyond p_2 (p_1>p_2) and air flows from chamber I to chamber II. So pressure changes at chambers I, II, III are as follows:

$$\frac{\mathrm{d}p_1}{\mathrm{d}t}=\frac{R\theta_1}{V_1}\left(G_{1\mathrm{i}}-G_{1\mathrm{o}}-G_{2\mathrm{i}}\right), \tag{11}$$

$$\frac{\mathrm{d}p_2}{\mathrm{d}t}=\frac{R\theta_2}{V_2}G_{2\mathrm{i}}, \tag{12}$$

$$\frac{\mathrm{d}p_3}{\mathrm{d}t}=\frac{R\theta_3}{V_3}\left(-G_{3\mathrm{o}}\right). \tag{13}$$

In period *c*, p_1 drops gradually. In period *d*, right operating chamber drops to p_{a}. Pressure changes at chambers I, II, III are as follows:

$$\frac{\mathrm{d}p_1}{\mathrm{d}t}=\frac{R\theta_1}{V_1}\left(-G_{1\mathrm{o}}+G_{2\mathrm{o}}\right), \tag{14}$$

$$\frac{\mathrm{d}p_2}{\mathrm{d}t}=\frac{R\theta_2}{V_2}\left(-G_{2\mathrm{o}}\right), \tag{15}$$

$$\frac{\mathrm{d}p_3}{\mathrm{d}t}=\frac{R\theta_3}{V_3}\left(G_{3\mathrm{i}}-G_{3\mathrm{o}}\right). \tag{16}$$

Considering the reference valve of Table 2 and coefficient Table 3, we can make the basic equations shown above dimensionless. The non-dimensional equation of motion can be written as follows, for the period of *a*, Eqs. (8)–(10) are made dimensionless:

$$\frac{\mathrm{d}p_1^*}{\mathrm{d}t^*}=G_{1\mathrm{i}}{}^*-k_1G_{1\mathrm{o}}{}^*+k_1k_{\mathrm{coin1}}k_2G_{2\mathrm{o}}^*, \tag{17}$$

$$\frac{\mathrm{d}p_2^*}{\mathrm{d}t^*}=-k_2k_{\mathrm{coin2}}G_{2\mathrm{o}}^*, \tag{18}$$

$$\frac{\mathrm{d}p_3{}^*}{\mathrm{d}t^*}=-k_3\frac{T_{\mathrm{r}}}{T_{\mathrm{r3}}}G_{3\mathrm{o}}^*. \tag{19}$$

For period *b*, Eqs. (11)–(13) are made dimensionless:

$$\frac{\mathrm{d}p_1^*}{\mathrm{d}t^*}=G_{1\mathrm{i}}^*-k_1G_{1\mathrm{o}}^*-k_{\mathrm{coin1}}k_1G_{2\mathrm{i}}^*, \tag{20}$$

$$\frac{\mathrm{d}p_2^*}{\mathrm{d}t^*}=k_{\mathrm{coin2}}G_{2\mathrm{i}}^*, \tag{21}$$

$$\frac{\mathrm{d}p_3^*}{\mathrm{d}t^*}=-k_3\frac{T_{\mathrm{r}}}{T_{\mathrm{r3}}}G_{3\mathrm{o}}^*. \tag{22}$$

For periods *c* and *d*, Eqs. (14)–(16) are made

dimensionless:

$$\frac{\mathrm{d}p_1^*}{\mathrm{d}t^*} = -k_1 G_{1o}^* + k_{coin1} k_2 k_1 G_{2o}^*, \tag{23}$$

$$\frac{\mathrm{d}p_2^*}{\mathrm{d}t^*} = -k_2 k_{coin2} G_{2o}^*, \tag{24}$$

$$\frac{\mathrm{d}p_3^*}{\mathrm{d}t^*} = \frac{T_r}{T_{r3}}\left(G_{3i}^* - k_3 G_{3o}^*\right). \tag{25}$$

Table 2. Reference valve and non-dimensional variable

Variable	Reference Variable	Description	Non-Dimensional variable
Pressure	p_s	Pressure supply	$p^* = \frac{p}{p_s}$
Time	$t_r = \frac{V}{R\theta_a \rho_0 C}\sqrt{\frac{\theta_a}{\theta_0}}$	Time to fill up a chamber (V) through a throttle (C) at a mass flow of G_{max}	$t^* = \frac{t}{t_r}$
Air Mass Flow	$G_{max} = \rho_0 C p_s \sqrt{\frac{\theta_0}{\theta_a}}$	The maximum mass flow through a throttle(C) at supply pressure of p_s	$G^* = \frac{G}{G_{max}}$

Table 3. Coefficient description

Symbol	Expression
k_{coin1}	C_{2i} / C_{1o}
k_{coin2}	t_r / t_{r2}
k_1	C_{1o} / C_{1i}
k_2	C_{2o} / C_{2i}
k_3	C_{3o} / C_{3i}

3.2.2 Comparison of simulation and experiment results

Table 4 shows the system parameters measured. It can be seen in Fig. 7 that there is a good agreement between experimental and simulation results.

Table 4. System parameters

Parameters of system for simulation	
Parameter	Value
Reference time t_r/s	0.01
Reference time t_{r2}/s	0.15
Reference time t_{r3}/s	0.55
Coefficient k_{coin1}	0.01
Coefficient k_{coin2}	0.07
Coefficient k_2	0.26
Coefficient k_3	0.38
Coefficient k_1	0.98
Differential pressure Δp/MPa	0.04
Response time t_{rsp}/s	0.01
Parameters of system components	
Parameter	Value
Supply pressure p_s/MPa	0.8
Pipe volume V_1/cm^3	5.65
Pipe volume V_2/cm^3	0.96
Pipe volume V_3/cm^3	5.61
Flow conductance C_{1o}/(dm^3 • s^{-1} • MPa^{-1})	6.2
Flow conductance C_{2o}/(dm^3 • s^{-1} • MPa^{-1})	0.016
Flow conductance C_{3i}/(dm^3 • s^{-1} • MPa^{-1})	0.1
Flow conductance C_{1i}/(dm^3 • s^{-1} • MPa^{-1})	6.4
Flow conductance C_{2i}/(dm^3 • s^{-1} • MPa^{-1})	0.062
Flow conductance C_{3o}/(dm^3 • s^{-1} • MPa^{-1})	0.038

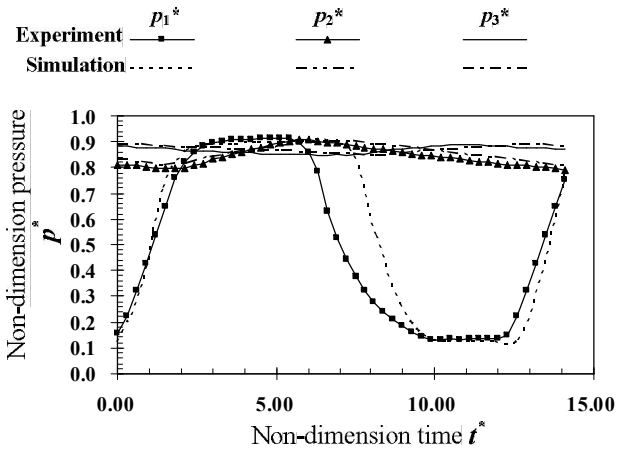

Fig. 7. Experimental and simulation results

There are differences between experimental and simulation results for the pressure response of chamber I, because it is assumed that the valve switches at constant speed, while in fact the motion of the valve is complicated. Above all, frequency and duty ratio are predicted well by the simulation. The absolute error of frequency is 1% and duty ratio is 12%. It can be found that C_{3i} is different from C_{1i}, both of which are the conductance of the valve(should be the same) in Table 4, because it is supposed that the valve port opens completely after switching, while in fact it may not opens completely.

3.3 System parameter design

In the last section, the outputs (frequency and duty ratio) of the self-oscillated system are predicted. There may be a function between outputs and system parameters. In this section, the function will be studied, which may be described as $(V, C) = F(f, \alpha)$.

The following definition can be made.

Definition (a): T is period of self-oscillated system, and $T = \Delta t_a + \Delta t_{b1} + t_0 + t_1 + 2t_{rsp}$.

Definition (b): f is oscillation frequency of system.

Definition (c): α is duty ratio.

To simplify the model, the following assumptions are made.

Assumption (a): The flow conductance from chamber II to chamber I is much smaller than from chamber III to atmosphere. The mass flow from chamber II to chamber I is small enough to disregard comparing with from chamber III to atmosphere, i.e., $k_{\text{coin1}} \ll 1$.

Assumption (b): The time taken to fill up chamber I is much smaller comparing with fill up chamber II, i.e., $k_{\text{coin2}} \ll 1$.

Assumption (c): The time taken to fill up chamber I is much smaller comparing with fill up chamber III, i.e., $t_{\text{r}} \ll t_{\text{r3}}$.

With these three assumptions the main stream and branches (Fig. 5) are defined. The mass flow in the main stream is times more than in branches. So the response of pressure in main stream is times faster than in branches. Assumptions (d) p_{work}^{*} >0.5 p_{a}^{*}<0.25 and Δp^{*}<0.5 as Fig. 6 shows.

3.3.1 Simplification of the model

For period a ([0, t_a^{*}]), comparing the magnitudes of teams in Eq. (17), the right third team is much smaller than the former teams with Assumption (a). So Eq. (17) can be rewritten as

$$\frac{\mathrm{d}p_1^{*}}{\mathrm{d}t^{*}} = G_{1\text{i}}^{*} - k_1 G_{1\text{o}}^{*}. \tag{26}$$

Comparing the magnitude of the first right team in Eq. (18) with the first two teams in Eq. (17), the former is much smaller than latter with Assumption (b). The variation of pressure in chamber II is so small comparing with chamber I that it can be regard to be constant. Similarly the variation of pressure in chamber III is disregarded. So Δt_{a} in Fig. 6 is decided by Eq. (26).

The period of b can be divided into two parts, for the part b_1 in Fig. 6, the pressure of chamber I rises from p^{*}_{work} to p_0^{*}. For part b_2, the pressure of chamber I keeps to be a constant (p_0^{*}).

For part b_1 ([t_a^{*}, t_{b1}^{*}]), the different from period a is flow direction between chambers I and II. The analysis of period a can be preformed to part b_1. Time period Δt_{b1} in Fig. 6 is decided by Eq.(26).

For part b_2 ([t_{b1}^{*}, t_{b2}^{*}]), the pressure in chamber I gradually becomes saturation. So the variation of pressure is disregarded in the period. The pressure difference between chamber I and II becomes large gradually. When it comes to time point t_{b2} in Fig. 6 the valve begin to switch. Time period t_1 in Fig. 6 is decided by Eqs. (21), (22).

Comparing the magnitude of right team in Eq. (21) with right two teams in Eq. (26), the former is much smaller than latter. The rate of pressure variation in Eq. (26) is much faster than in Eq. (21). As a result, the time period Δt_a^{*} is so small comparing with t_1 that the relationship between them can be written as

$$\frac{\Delta t_a^{*}}{t_1^{*}} \ll 1. \tag{27}$$

The same analysis is preformed to part b_1, the following is obtained:

$$\frac{\Delta t_{b1}^{*}}{t_1^{*}} \ll 1. \tag{28}$$

With Definition (a) and Eqs. (27), (28), the following is obtained:

$$T^{*}\alpha \doteq t_1^{*} + t_{\text{rsp}}^{*}. \tag{29}$$

With the analysis above, the pressure of chamber I is regarded to be p_0^{*}. So Eq. (26) can be written as

$$G_{1\text{i}}^{*} = k_1 G_{1\text{o}}^{*}. \tag{30}$$

On Assumption (d) (p^{*}_{work}>0.5), there are

$$G_{1\text{i}}^{*} = 2\sqrt{p_1^{*}\left(1 - p_1^{*}\right)}, \tag{31}$$

$$G_{1\text{o}}^{*} = p_1^{*}. \tag{32}$$

Eqs. (31) and (32) are substituted into Eq. (30), then the following can be obtained:

$$p_0^{*} = \frac{4}{4 + k_1^{2}}. \tag{33}$$

On Assumption (d) (p^{*}_{work}>0.5, Δp^{*}<0.5), the mass flow into the chamber II and the mass flow out the chamber III can be respectively written as follows:

$$G_{2\text{i}}^{*} = p_0^{*} \bullet 2\sqrt{\frac{p_2^{*}}{p_0^{*}}\left(1 - \frac{p_2^{*}}{p_0^{*}}\right)}, \tag{34}$$

$$G_{3\text{o}}^{*} = p_3^{*}. \tag{35}$$

Eq. (34) is linearized at work point p_2^{*}= p_{work}^{*} and substituted into Eq. (20), then the following can be obtained:

$$\frac{\mathrm{d}p_2^{*}}{\mathrm{d}t^{*}} = -\frac{2p_{\text{work}}^{*} - p_0^{*}}{\sqrt{p_{\text{work}}^{*}\left(p_0^{*} - p_{\text{work}}^{*}\right)}} k_{\text{coin2}}\left(p_2^{*} - \frac{p_0^{*} p_{\text{work}}^{*}}{2p_{\text{work}}^{*} - p_0^{*}}\right). \tag{36}$$

t_1^* is obtained by integrating Eq. (36) as follows:

$$t_1^* = -\frac{1}{k_{coin2}} \frac{\sqrt{p_{work}^* \left(p_0^* - p_{work}^*\right)}}{2p_{work}^* - p_0^*} \ln 1 - \frac{2p_{work}^* - p_0^*}{2p_0^* - 2p_{work}^*} \bullet \frac{\Delta p^*}{p_{work}^*}. \quad (37)$$

Substituting Eq. (35) into Eq. (22), we can obtain:

$$\frac{dp_3^*}{dt^*} = -k_3 \frac{T_r}{T_{r3}} p_3^*. \quad (38)$$

t_1^* is obtained by integrating Eq. (38) as follows:

$$t_1^* = \frac{1}{k_3} \frac{T_{r3}}{T_r} \ln 1 + \frac{\Delta p^*}{p_{work}^*}. \quad (39)$$

For period c ($[t_b^*, t_c^*]$), with the same analysis as period a, Eq. (23) can be rewritten as

$$\frac{dp_1^*}{dt^*} = G_{1i}^* - k_1 G_{1o}^*. \quad (40)$$

Δt_c in Fig. 6 is decided by Eq. (40). With the magnitude analysis, the time period Δt_c^* is so small comparing with t_0 that the relationship between them can be written as

$$\frac{\Delta t_c^*}{t_0^*} \ll 1. \quad (41)$$

With Defining (a) and Eq. (40), the following can be obtained:

$$T^* \left(1 - \alpha\right) = t_0^* + t_{rsp}^*. \quad (42)$$

For period d ($[t_c^*, t_{d1}^*]$), the compressed air in chamber I is discharged completely. The pressure of chamber I is regarded as same as atmosphere (p_a^*). On Assumption (d) ($p_{work}^* > 0.5$), the mass flow out the chamber II and the mass flow into/out the chamber III can be written as follows:

$$G_{2o}^* = p_2^*, \quad (43)$$

$$G_{3i}^* = 2\sqrt{p_3^* \left(1 - p_3^*\right)}, \quad (44)$$

$$G_{3o}^* = p_3^*. \quad (45)$$

Eq. (44) is linearized at work point $p_3^* = p_{work}^*$ and substituted into Eq. (25) with Eq. (45), the following is obtained:

$$\frac{dp_3^*}{dt^*} = -\frac{2p_{work}^* - 1}{\sqrt{p_{work}^* \left(1 - p_{work}^*\right)}} \frac{t_r}{t_{r3}} \left(p_3^* - \frac{p_{work}^*}{2p_{work}^* - 1}\right) - k_3 \frac{t_r}{t_{r3}} p_3^*. \quad (46)$$

t_0^* is obtained by integrating Eq. (46) as follows:

$$t_0^* = \frac{-\sqrt{p_{work}^* \left(1 - p_{work}^*\right)}}{2p_{work}^* - 1 + k_3 \sqrt{p_{work}^* \left(1 - p_{work}^*\right)}} \frac{t_{r3}}{t_r} \ln 1 - \frac{2p_{work}^* - 1 + k_3 \sqrt{p_{work}^* \left(1 - p_{work}^*\right)}}{2 - 2p_{work}^* - k_3 \sqrt{p_{work}^* \left(1 - p_{work}^*\right)}} \bullet \frac{\Delta p^*}{p_{work}^*}. \quad (47)$$

Substituting Eq. (43) into Eq. (24), we can obtain:

$$\frac{dp_2^*}{dt^*} = -k_2 k_{coin2} p_2^*. \quad (48)$$

t_0^* is obtained by integrating Eq. (48) as follows:

$$t_0^* = \frac{1}{k_2} \frac{1}{k_{coin2}} \ln 1 + \frac{\Delta p^*}{p_{work}^*}. \quad (49)$$

Substituting Eqs. (37), (39) into Eq. (29), respectively, we can obtain:

$$k_2 = \frac{\frac{T^* \alpha - t_{rsp}^*}{T^* \left(1 - \alpha\right) - t_{rsp}^*} \bullet \ln 1 + \frac{\Delta p^*}{p_{work}^*}}{-\frac{\sqrt{p_{work}^* \left(p_0^* - p_{work}^*\right)}}{2p_{work}^* - p_0^*} \ln 1 - \frac{2p_{work}^* - p_0^*}{2p_0^* - 2p_{work}^*} \bullet \frac{\Delta p^*}{p_{work}^*}}, \quad (50)$$

$$t_{r3} = t_r \left(T^* \alpha - t_{rsp}^*\right) \bullet \frac{-\frac{\sqrt{p_{work}^* \left(p_0^* - p_{work}^*\right)}}{2p_{work}^* - p_0^*}}{\ln 1 - \frac{2p_{work}^* - p_0^*}{2p_0^* - 2p_{work}^*} \bullet \frac{\Delta p^*}{p_{work}^*}}. \quad (51)$$

Substituting Eqs. (47), (49) into Eq. (42), respectively, we can obtain:

$$\frac{T^* \left(1 - \alpha\right) - t_{rsp}^*}{T^* \alpha - t_{rsp}^*} \ln 1 + \frac{\Delta p^*}{p_{work}^*} = \frac{-k_3 \sqrt{p_{work}^* \left(1 - p_{work}^*\right)}}{2p_{work}^* - 1 + k_3 \sqrt{p_{work}^* \left(1 - p_{work}^*\right)}} \ln 1 - \frac{2p_{work}^* - 1 + k_3 \sqrt{p_{work}^* \left(1 - p_{work}^*\right)}}{2 - 2p_{work}^* - k_3 \sqrt{p_{work}^* \left(1 - p_{work}^*\right)}} \bullet \frac{\Delta p^*}{p_{work}^*}, \quad (52)$$

$$t_{r3} = t_r \frac{\left(T^* \alpha - t_{rsp}^*\right) \bullet k_3}{\ln\left(1 + \Delta p^* / p_{work}^*\right)}. \quad (53)$$

The parameters (t_{r2}, t_{r3}, k_2, k_3) are solved based on Eqs. (51)–(54) with specified f and α. The parameters determine dimensions of pipes and throttles in Table 5 are obtained according to t_{r2}, t_{r3}, k_2 and k_3.

3.4 Experiment result

Table 5 shows an example for designing the system. It can be seen in Fig. 8 that the system works with the duty

ratio and frequency almost as designed to. The absolute error of duty ratio increases from 7% to 33% as frequency increases, one of the reasons for this is the assumption that the valve switches at uniform velocity, so there is a difference between calculation and experiment in response time of air operated valve. So when the period of the system (T) becomes small the difference increases and cannot be disregarded. Another, Assumptions (a), (b) and (c) cannot be satisfied practically. So when the period of the system becomes small, Δt_a^* and Δt_c^* cannot be overlook.

Table 5. Example for system design

Design objective		
Parameter	Value	
Oscillation frequency f/Hz	6	13
Oscillation duty ratio α/%	50	30
Selected parameters		
Parameter	Value	
Supply pressure p_s/MPa	0.8	
Differential pressure Δp/MPa	0.04	
Flow conductance C_{1o}/(dm^3 • s^{-1} • MPa^{-1})	6.2	
Flow conductance C_{1i}/(dm^3 • s^{-1} • MPa^{-1})	6.4	
Flow conductance C_{3i}/(dm^3 • s^{-1} • MPa^{-1})	0.1	
Response time t_{rsp}/s	0.01	
Calculated parameters		
Parameter	Value	
Reference time t_{r2}/s	0.54	0.15
Reference time t_{r3}/s	0.84	0.61
Coefficient k_2	0.60	0.25
Coefficient k_3	0.39	0.36
Coefficient k_{coin1}	0.01	
Coefficient k_{coin2}	0.03	0.07
Parameters of system components		
Parameter	Value	
Pipe volume V_1/cm^3	10.5	6.91
Pipe volume V_2/cm^3	3.42	0.97
Pipe volume V_3/cm^3	8.61	6.19
Flow conductance C_{2i}/(dm^3 • s^{-1} • MPa^{-1})	0.062	
Flow conductance C_{2o}/(dm^3 • s^{-1} • MPa^{-1})	0.037	0.02
Flow conductance C_{3o}/(dm^3 • s^{-1} • MPa^{-1})	0.039	0.036

4 Conclusions

(a) The paper presents an innovative air blowing system blowing pulse flow. The method of pulse blowing is proved to save energy comparing with the continuous method. The experiment result shows that pulse blowing system consumes less air and time.

(b) The influence of pulse frequency and duty ratio on energy consumption is studied. Optimum parameters are obtained and applied to save energy by 70%.

(c) The paper presents a pneumatic self-oscillated system based on air operated valve. By simulating the behavior of the system, the important parameters of frequency and duty ratio is calculated.

(d) The paper presents a method to design the system with specified pulse frequency and duty ratio. The pressure differential equations of chamber I and II are coupled. The equations are difficult to solve. The parameters of k_{coin1} and k_{coin2} are presented to indicate coupling degree. If coupling degree is small the design method works.

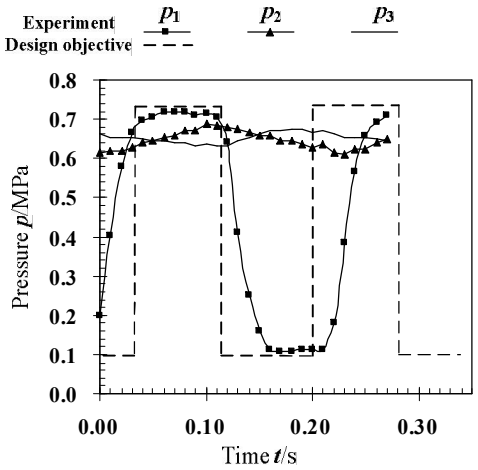

(a) Objective frequency is 6 Hz

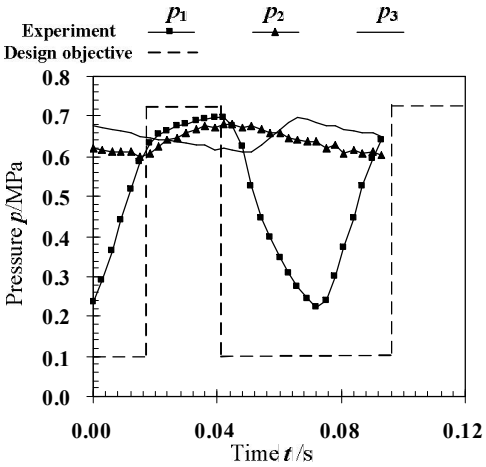

(b) Objective frequency is 13 Hz

Fig. 8. Pressure response of chambers I, II, III

References

[1] Japan Fluid Power Association. *Report on energy conservation of air compressor system in 2001*[R]. Tokyo, 2002.

[2] ONEYAMA N. The actual situation and problems on energy savings of pneumatic system[J]. *Journal of Fluid Power System*, 2001, 32(4): 231–236 .

[3] Van Leer (UK) Ltd. *Compressed air savings by leakage reduction and efficient air nozzles*[G]. IEA, 2001, Result 402.

[4] CHAHINE G L, JOHNSON J, FREDERICK G S. *Self resonating pulsed water jets for aircraft coating removal: feasibility study*[R]. HYDRONAUTICS, Incorporated Technical Report 826889, 1982.

[5] CHAHINE G L, JOHNSON J, FREDERICK G S. Cleaning and cutting with self-resonating pulsed water jets[C]//*Proceedings of the Second US Water Jet Conference*, Missouri, United State, 1983: 195–207.

[6] WANG Xunming, JAO Lei, WANG Leqin. Numerial simulation of self-excited oscillation pulsed jet and analysis of parameters' influence[J]. *Journal of Zhejiang University (Engineer Science)*, 2005, 39(9): 1 450–1 454.

[7] SENOO Mitsuru. Reduction of air consumption by appropriate

air blow system[J]. *Journal of Hydraulics and Pneumatic*, 1999, 38(6): 5–10.

[8] KOKOROZASI Kuma. *Rational utilization of air blow to reduce air consumption, collected cases of energy conservation in 2000*[R]. Tokyo: Energy Conservation Center, 2000.

[9] ONEYAMA N. *Energy saving for pneumatic system*[R]. Tokyo: Energy Conservation Center, 2003.

[10] YANG Geunyoung, LEE Joon Sik, CHOI Mansoo, et al. Experimental study of slot jet impingement cooling on concave surface: Effects of nozzle configuration and curvature[J]. *International Journal of Heat and Mass Transfer*, 1999, 42(12): 2 199–2 209.

[11] CAI Maolin, KENJI Kawashima, TOSHIHARU Kagawa. Power assessment of flowing compressed air[J]. *Journal of Fluids Engineering, Transactions of the ASME*, 2006, 128(2): 402–405.

[12] The Japan Hydraulic and Pneumatic Society. *Manual of hydraulics and pneumatics*[M]. Tokyo: Ohmu Ltd., 1989.

Biographical notes

CAI Maolin, born in 1972, is currently a professor and a PhD candidate supervisor in School of Automation Science and Electrical Engineering, Beihang University, China. His main research interests include the energy saving, measurement, simulation, and control of pneumatic system.
E-mail: caimaolin@gmail.com

XU Weiqing, born in 1984, is currently a PhD candidate in School of Automation Science and Electrical Engineering, Beihang University, China. He received his bachelor degree from Hunan University, China, in 2003. His research interests include pneumatic blowing system.
E-mail: xwqyyl@163.com